Rapidity- and azimuthally-dependent femtoscopy in $\sqrt{s_{\mathrm{NN}}} = 5.02$ TeV p+Pb collisions with *ATLAS*

Phys. Rev. C 96 (2017) 064908
ATLAS-CONF-2017-008

Michael (Felix) Clark

On behalf of the ATLAS collaboration

XIII Workshop on Particle Correlations and Femtoscopy
Kraków, Poland

22 May, 2018

COLUMBIA UNIVERSITY
IN THE CITY OF NEW YORK

Motivation

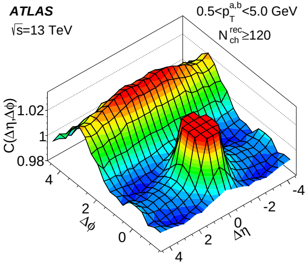

Phys. Rev. Lett. **116**, 172301
Phys. Rev. Lett. **110**, 182302

- “ridge” is observed in p+Pb (below) and pp (left) collisions – near-side long-range angular correlation; explained by hydrodynamics
- the applicability of hydro in small systems is controversial
- useful to measure source size as function of centrality, momentum, azimuthal angle

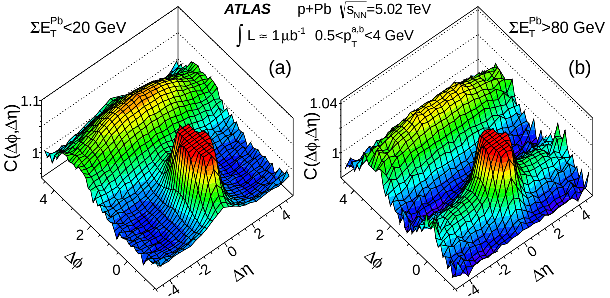

Introduction

- Momentum-space 2-particle correlation functions,

$$C(\mathbf{p}_1, \mathbf{p}_2) \equiv \frac{\frac{dN_{12}}{d^3\mathbf{p}_1 d^3\mathbf{p}_2}}{\frac{dN_1}{d^3\mathbf{p}_1}\frac{dN_2}{d^3\mathbf{p}_2}} ,$$

are sensitive to the 2-particle source density function $S_{\mathbf{k}}(\mathbf{r})$:

$$C_{\mathbf{k}}(\mathbf{q}) = \int d^3r\, S_{\mathbf{k}}(\mathbf{r})\, |\psi_{\mathbf{q}}(\mathbf{r})|^2 \ .$$

$\mathbf{r}$ is the displacement between the 2 particles at freezeout,
$\mathbf{k} = (\mathbf{p}_1 + \mathbf{p}_2)/2$ is the average pair momentum, and $\mathbf{q} = (\mathbf{p}_1 - \mathbf{p}_2)$ is the relative momentum.

- Background $\frac{dN_1}{d^3\mathbf{p}_1}\frac{dN_2}{d^3\mathbf{p}_2}$ is formed by event-mixing within intervals of centrality and longitudinal position of the collision vertex.

Introduction

- Bose-Einstein correlations between identical pions provide particularly good resolution of the source function.
  - For identical non-interacting bosons, $C_{\mathrm{BE}}(\mathbf{q}) = 1 + \mathcal{F}[S(\mathbf{r})]$.
- $C(\mathbf{q})$ is fit to some function to extract characteristic length scales of $S(\mathbf{r})$, which are referred to as the *HBT radii*.
- Bowler-Sinyukov form is used for the full correlation function:

$$C_{\mathrm{full}}(\mathbf{q}) = [(1-\lambda) + \lambda K(q_{\mathrm{inv}}) C_{\mathrm{BE}}(\mathbf{q})]\, \Omega(\mathbf{q}) \ ,$$

  - $K(q_{\mathrm{inv}})$: Coulomb interactions between the pions
  - $\Omega(\mathbf{q})$: non-femtoscopic background features (jet fragmentation)
  - λ: parameter $0 \leq \lambda \leq 1$ that accounts for mis-identified pions, coherent emission, and long-lived decays ($\lambda = 1$ in an idealized limit; typically 0.8–1)

Introduction

The Bertsch-Pratt coordinate system is used, which is boosted to the longitudinal co-moving frame (LCMF) of each pair.

R_{out}: along k_{T}

R_{side}: other transverse direction

R_{long}: longitudinal (boosted to LCMF)

The Bose-Einstein part of the correlation function is fit to an quasi-ellipsoid exponential:

$$C_{\text{BE}}(\mathbf{q}) = 1 + \exp\left(-\left\|R\mathbf{q}\right\|\right)$$

$$R = \begin{pmatrix} R_{\text{out}} & R_{\text{os}} & R_{\text{ol}} \\ R_{\text{os}} & R_{\text{side}} & 0 \\ R_{\text{ol}} & 0 & R_{\text{long}} \end{pmatrix}$$

with either $R_{\text{os}} = 0$ or $R_{\text{ol}} = 0$.

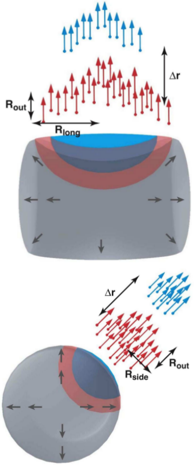

Ann. Rev. Nucl. Part. Sci. 55 (2005) 357

ATLAS inner detector

- pixel detector - 82 million silicon pixels
- semiconductor tracker - 6.2 million silicon microstrips
- transition radiation tracker - 350k drift tubes
- $2\,\mathrm{T}$ axial magnetic field

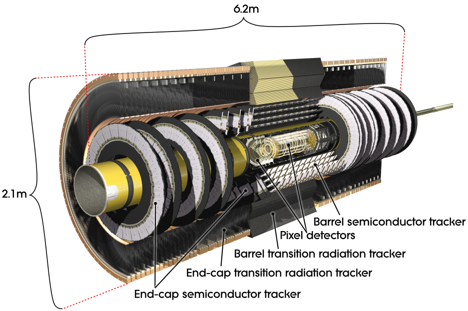

Reconstructed tracks from $|\eta| < 2.5$ and $p_{\mathrm{T}} > 0.1$ GeV

Data selection

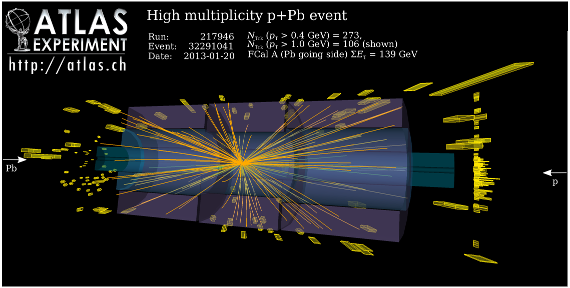

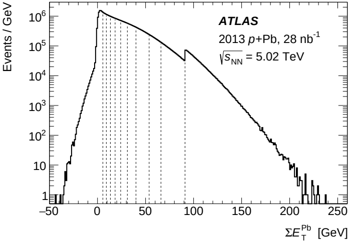

- 2013 p+Pb run from the LHC at $\sqrt{s_{\mathrm{NN}}} = 5.02$ TeV
- 28 nb^{-1} minimum bias data sample
- centrality, experimental proxy for impact parameter, determined from $\sum E_{\mathrm{T}}$ in the Pb-going side of forward calorimeter (right) at $-4.9 < \eta < -3.1$ ($y_{\mathrm{Pb}} < 0$, $y_p > 0$)

Pion identification

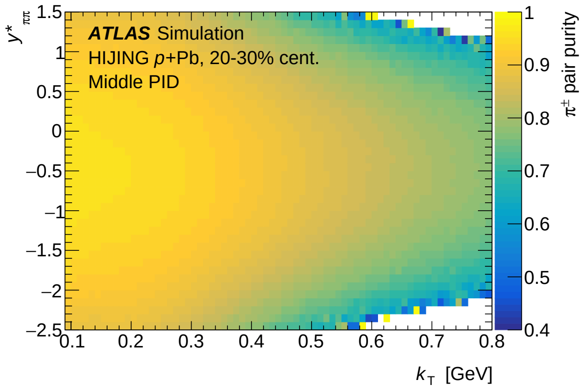

- Charged pions are identified using dE/dx measured from the charge deposited in pixel hits.
- The pair purity estimated from HIJING simulation is shown (left) as a function of pair k_{T} and $y^\star_{\pi\pi}$.

k_{T}: transverse component of the pair's average momentum

$y^\star_{\pi\pi} = y_{\pi\pi} - 0.465$: rapidity in the nucleon-nucleon centre-of-momentum frame

PRC **96** (2017) 064908

Jet fragmentation correlation

- significant background observed in the two-particle correlation function, also in HIJING which has no femtoscopic signal (top)
- suppressing hard processes by turning up minimum hard-scattering p_T ($p_T^{\mathrm{HS,min}}$) in HIJING causes the correlation to disappear (bottom)
- opposite-charge correlations also contain jet fragmentation correlations, but no BE enhancement

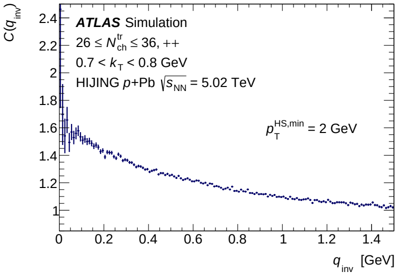

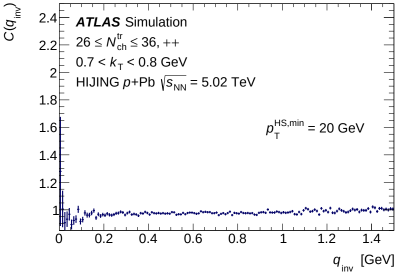

PRC **96** (2017) 064908

Jet fragmentation correlation

Common methods to account for this background include:

1. Using a double ratio, dividing by correlation function in Monte Carlo simulation: $C(q) = C^{data}(q)/C^{MC}(q)$.
   - MC tends to over-estimate the magnitude of the effect, skewing results significantly.
2. Partially describing the background shape using simulation and allowing additional free parameters in the fit.
   - Additional free parameters can bias the fits.

In this analysis the jet fragmentation is measured in opposite-charge pair data and a mapping is derived in Pythia 8 to predict the form in same-charge correlations (see PRC **96** (2017) 064908).

Summary of fitting procedure

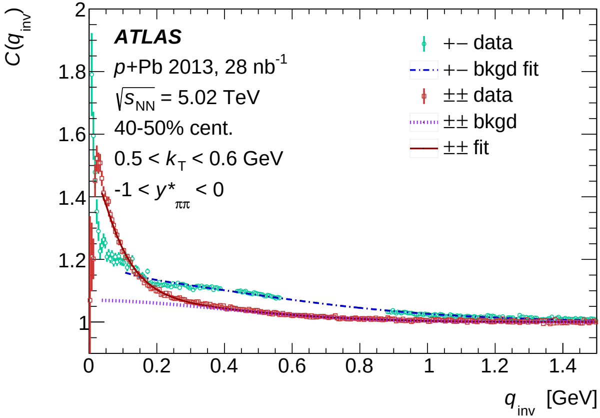

1. amplitude and width of opposite-charge correlation function are fit (blue dashed) from the opposite-charge pair distribution with resonances removed by mass cuts (teal points)
2. the results from $+-$ are used to fix $\pm\pm$ background (violet dotted)
3. source radii are extracted by fitting full correlation function $\pm\pm$ (dark red) taking into account jet background

PRC **96** (2017) 064908

Example fit to 3D correlation function

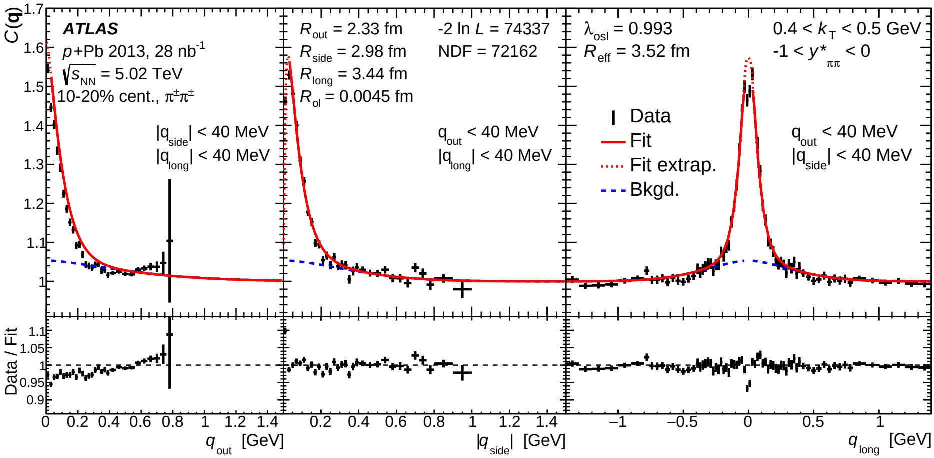

Fit works well globally ($\chi^2/\mathrm{d.o.f.} = 1.03$) but appears poor along q_{out} axis, where the tracks have the same outgoing angle. Moving just 1 or 2 bins along q_{side} or q_{long} helps significantly.

HBT radii vs. k_T

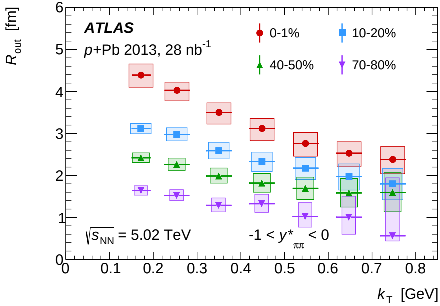

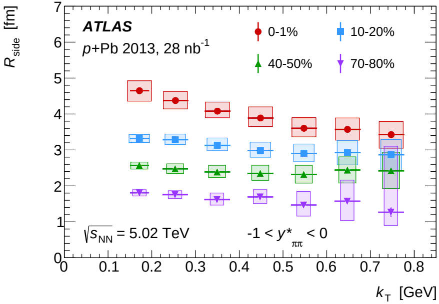

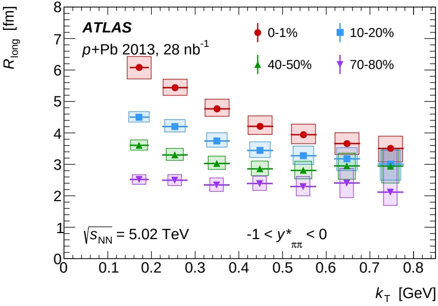

- decreasing size with rising k_T indicates collective expansion
- visible in central events; trend is diminished in peripheral
- $R_{out} < R_{side} < R_{long}$

PRC **96** (2017) 064908

HBT radii vs. $y^{\star}_{\pi\pi}$

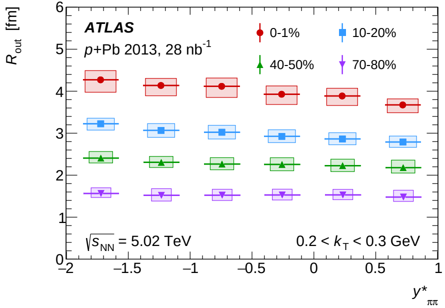

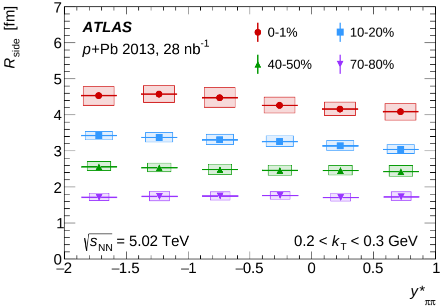

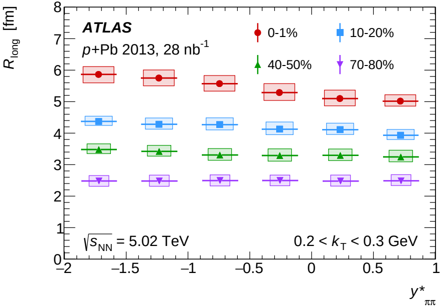

- *p* beam has positive rapidity; Pb beam has negative
- radii vs. $y^{\star}_{\pi\pi}$ are flat in peripheral, and larger on Pb-going side of central

PRC **96** (2017) 064908

HBT radii vs. local multiplicity

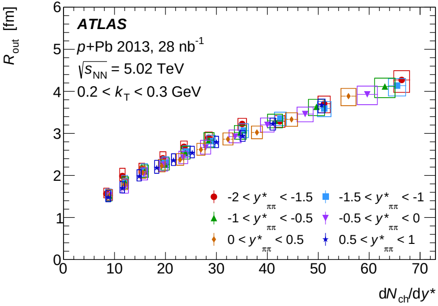

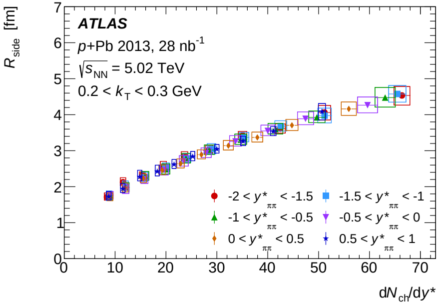

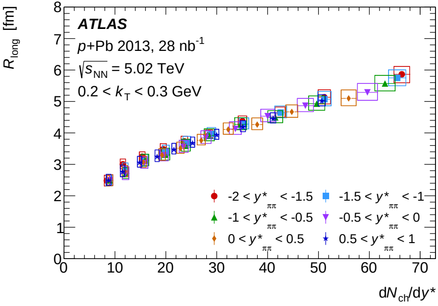

- radii are plotted against the local single-particle multiplicity in each centrality/rapidity interval
- HBT radii are tightly correlated with local multiplicity

PRC **96** (2017) 064908

Ratio of $R_{\mathrm{out}} / R_{\mathrm{side}}$

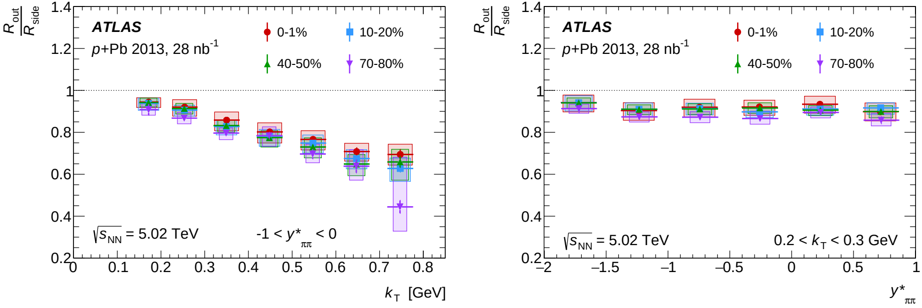

- in hydro models, R_{out} depends on the lifetime while R_{side} does not
- small ratio $R_{\mathrm{out}}/R_{\mathrm{side}}$ is indicative of “explosive” event
- steadily decreases with rising k_{T} and is constant over rapidity
- marginally larger in central events, but not significant

discussion in Ann. Rev. Nucl. Part. Sci. 55 (2005) 357
plots from PRC **96** (2017) 064908

Transverse area and volume elements

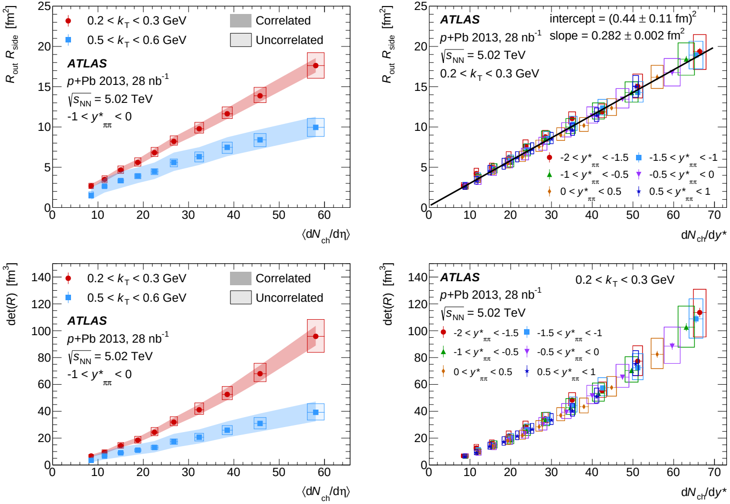

At low k_{T}, the transverse area element $R_{\mathrm{out}} R_{\mathrm{side}}$ scales linearly with multiplicity, indicating constant transverse areal density

PRC **96** (2017) 064908

out-long cross term: R_{ol}

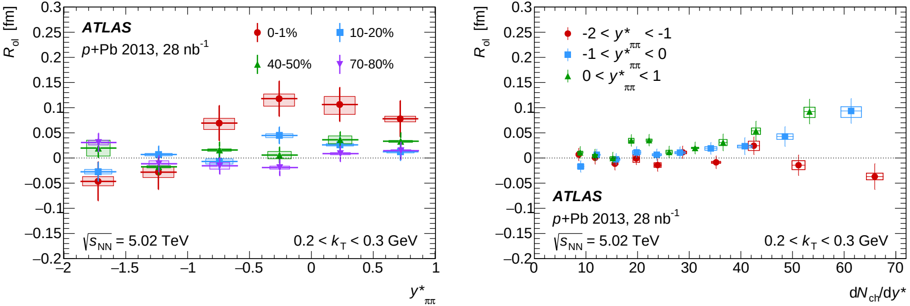

In *central events* on the *forward* side, there is strong evidence of a positive R_{ol} (5.1σ combined significance in 0–1% centrality)

- demonstrates breaking of boost invariance: z-asymmetry is manifest in proton-going side.
- requires both longitudinal and transverse expansion in hydrodynamic models

- first time this has been observed at RHIC/LHC

see theory comparison (agrees well): previous talk by Sebastian Bysiak

Azimuthal analysis

- HBT radii are also measured in central events (0–1%) as function of flow vector magnitude $|\vec{q}_2|$ and angle w.r.t. the 2nd-order event plane (EP) angle Ψ_2.

$$\vec{q}_2 \equiv |\vec{q}_2| e^{i2\Psi_2} = \frac{\sum_k E_{T,k} e^{i2\phi}}{\sum_k E_{T,k}}$$

- The analysis procedure is largely identical, with some exceptions:
  - high-multiplicity triggers included to improve statistics
  - inclusive in rapidity; differential in azimuthal angle w.r.t. Ψ_2
  - EP angles are aligned in event mixing
  - allowed cross term out-side (R_{os}) instead of out-long (R_{ol})
- 0th- and 2nd-order Fourier components are extracted, e.g.:

$$R_i = R_{i,0} + 2R_{i,2} \cos\left[2(\phi_k - \Psi_2)\right]$$

Azimuthal HBT in Au+Au at RHIC

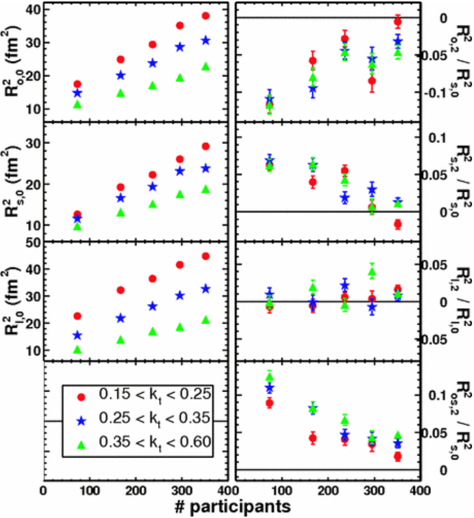

STAR (left) and PHENIX have measured the source size in Au+Au as function of azimuthal angle, and its Fourier components.

- $R_{\mathrm{out},2} < 0$
- $R_{\mathrm{side},2} > 0$
- $R_{\mathrm{long},2} \gtrsim 0$
- $R_{\mathrm{os},2} > 0$

These results are consistent with short-lived hydro. The source freezes out before its elliptic orientation is reversed by expansion.

Phys.Rev.Lett. 93 (2004) 012301

Azimuthal HBT in Pb+Pb at LHC

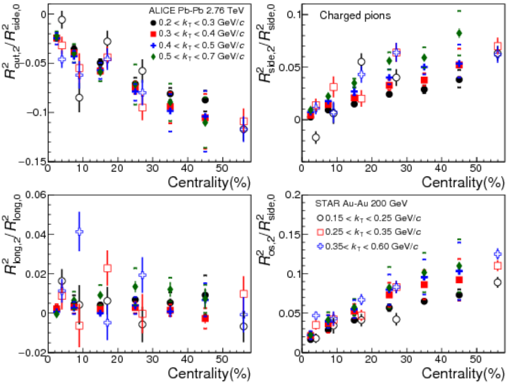

Phys. Rev. Lett. 118 (2017) 222301

ALICE has recently published a similar azimuthal result in Pb+Pb at the LHC.

- $R_{\text{out},2} < 0$
- $R_{\text{side},2} > 0$
- $R_{\text{long},2} \gtrsim 0$
- $R_{\text{os},2} > 0$

Results are still consistent with short-lived hydro.

later today: ALICE femtoscopy results by Magorzata Janik

Event plane resolution

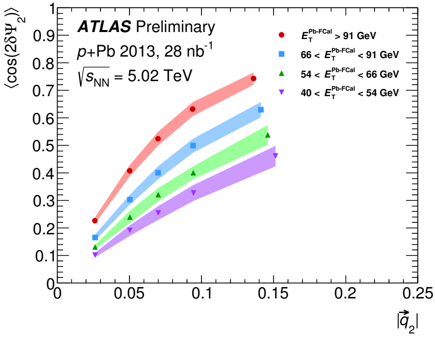

For these azimuthal results, only the points shown as red circles are used. The others are shown only to indicate the centrality dependence of EP resolution.

ATLAS-CONF-2017-008

- The 2nd-order event plane angle Ψ_2 is measured in the forward calorimeter at $\eta < -2.5$.
- The 2nd-order Fourier components of observables are decreased by factor of $\langle \cos(2\delta\Psi_2) \rangle$ (left).
- This is corrected by increasing bin-by-bin 2nd-order Fourier terms (which induces statistical correlations between radii in different azimuthal bins).

* Event-mixed distributions complicate the matter, but historically, and here, these have been corrected in the same way. (coffee break discussion)

$R_{\rm out}$: azimuthal dependence

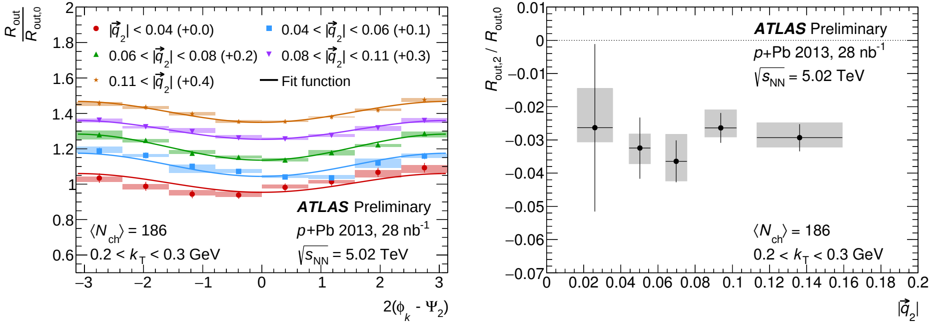

- in hydro, $R_{\rm out}$ couples to the lifetime directly
- sign of modulation indicates smaller in-plane size: $R_{\rm out,2} < 0$
- same orientation observed in A+A
  (note ATLAS uses $-\pi$ to π convention for ϕ_k)

ATLAS-CONF-2017-008

R_{side}: azimuthal dependence

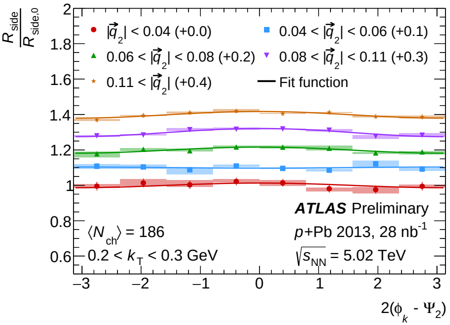

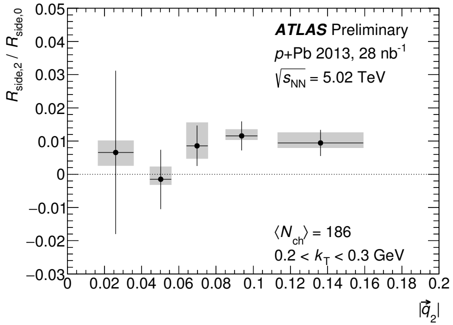

- R_{side} more purely geometrical radius
- sign of modulation also indicates smaller in-plane size: $R_{\mathrm{side},2} > 0$

ATLAS-CONF-2017-008

R_{long}: azimuthal dependence

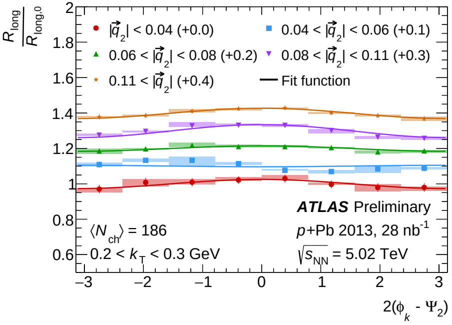

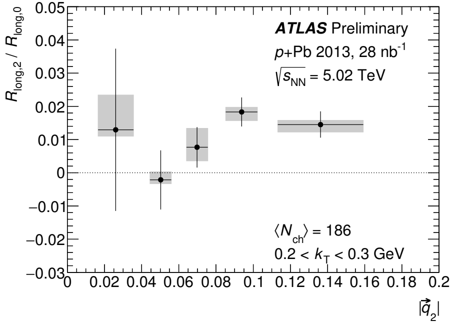

- enhanced longitudinal expansion in-plane: $R_{\mathrm{long},2} > 0$

ATLAS-CONF-2017-008

$R_{\rm os}$: azimuthal dependence

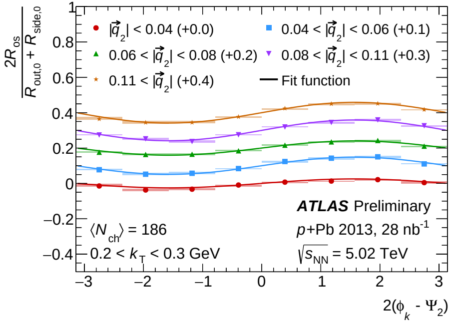

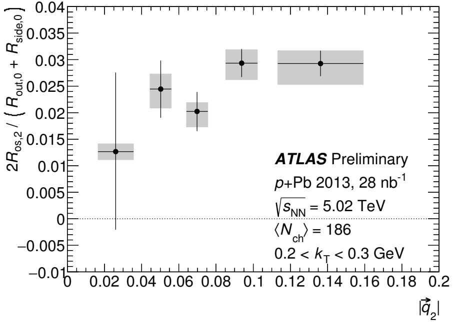

- fit to sine instead of cosine; no 0th-order term

$$R_{\rm os} = 2R_{{\rm os},2} \sin\left[2(\phi_k - \Psi_2)\right]$$

- normalized by 0th component of mean transverse radii
- also consistent with A+A observations: $R_{{\rm os},2} > 0$

$\det(R_T)$: azimuthal dependence

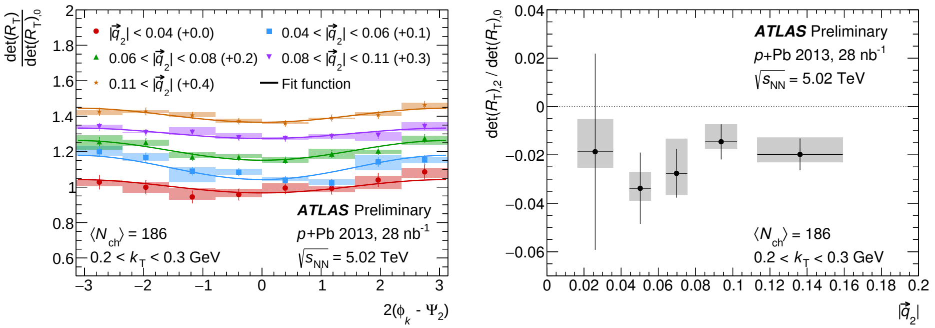

- $\det(R_T) = R_{out} R_{side} - R_{os}^2$
- transverse area of homogeneity region is slightly suppressed in-plane

ATLAS-CONF-2017-008

$\det(R)$: azimuthal dependence

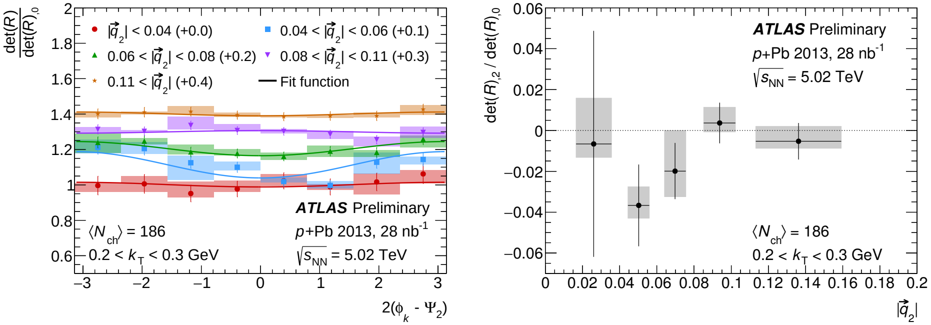

- modulation of volume element not able to be distinguished from zero

ATLAS-CONF-2017-008

Summary

- The freeze-out source size is measured in proton-lead collisions at 5 TeV, differential in centrality, transverse momentum, rapidity, and azimuthal angle from event plane.
- HBT radii in central events show a decrease with increasing k_{T}, which is qualitatively consistent with collective expansion. This trend is diminished in peripheral events.
- The source size is larger on Pb-going side of central events, but independent of rapidity (up to $|\eta| < 1.5$) in peripheral events.
- Azimuthal results in central collisions are consistent with short-lived hydrodynamic evolution.
- These include first observations of:
  - tight correlation between source size and local (rapidity-differential) multiplicity
  - positive R_{ol} on the proton-going side of central events
  - azimuthal modulation of source in central p+A

Thank you!

ATLAS

BACKUP SLIDES

Aside: Glauber-Gribov colour fluctuations (GGCF)

Number of nucleon participants N_{part} calculated with:

- Glauber model with constant cross section σ_{NN}
- Glauber-Gribov color fluctuation (GGCF) model, which allow σ_{NN} to fluctuate event-by-event

ω_σ parameterizes width of fluctuations

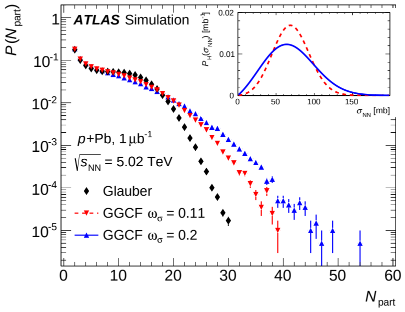

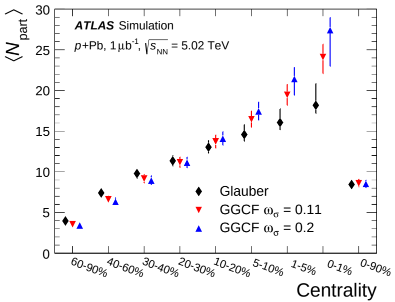

(above: N_{part} distributions and corresponding centrality)

see Eur. Phys. J. C (2016) 76:199

Volume–N_{part} scaling including color fluctuations

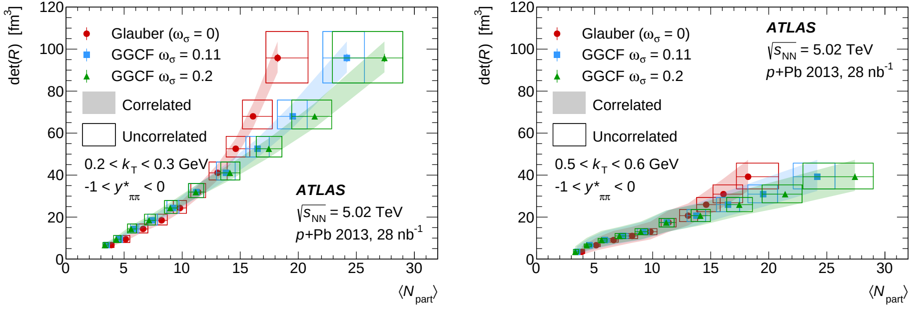

- volume scaling curvature with N_{part} is more modest when fluctuations in the proton's cross-section are accounted for
- exact linear scaling not necessary, but extreme deviations are difficult to explain
- shows that fluctuations in the nucleon-nucleon cross-section are crucial for understanding initial geometry of p+Pb collisions

PRC **96** (2017) 064908

Comparison to ALICE p+Pb results

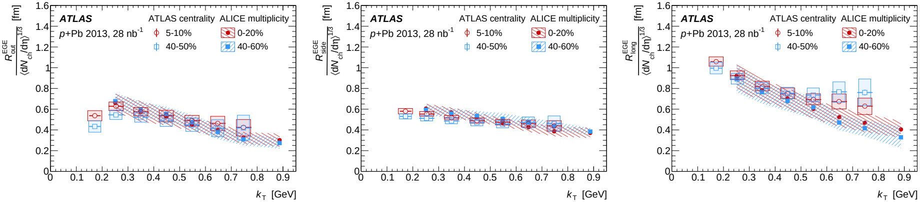

"EGE" (exponential-gauss-exponential) results compared between ATLAS and ALICE. This form is not used for the main ATLAS results, and is shown here for comparison only.

Comparable rapidity windows are used, and they are scaled by $\langle \mathrm{d}N_{\mathrm{ch}}/\mathrm{d}\eta \rangle^{1/3}$ to scale out differences in centrality definition.

Example fit to invariant correlation function

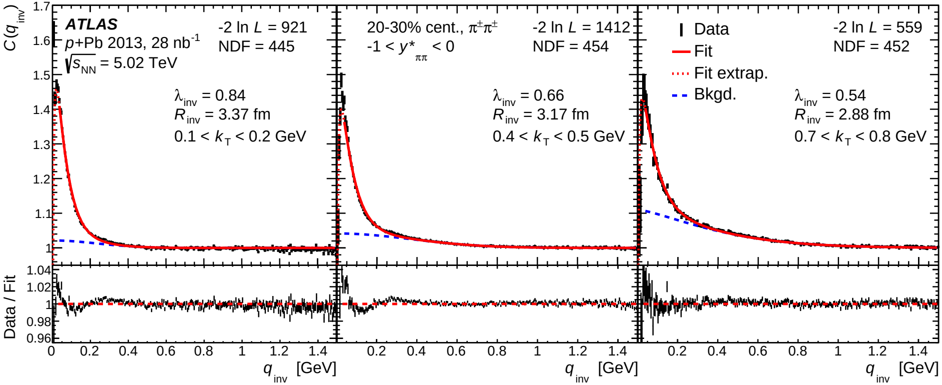

fit and background estimation typically describe $C(q_{\mathrm{inv}})$ quite well

Results for invariant radius R_{inv}

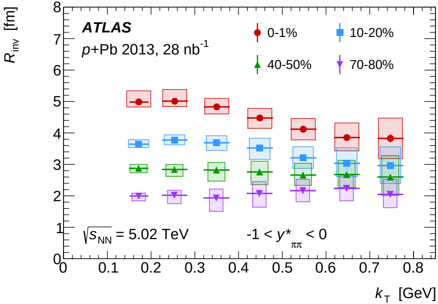

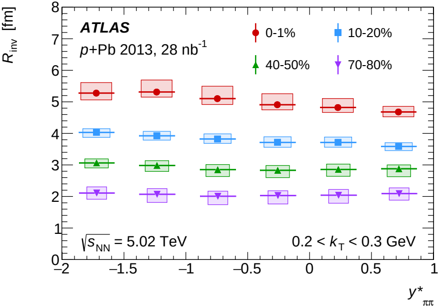

Decrease with rising k_{T} in central collisions, consistent with collective behavior. This feature disappears in peripheral collisions.

Radii increase in Pb-going direction of central events. Peripheral are constant with rapidity.

N.B. Widths of boxes in these plots vary only for visual clarity.

PRC **96** (2017) 064908

Results for invariant radius R_{inv}

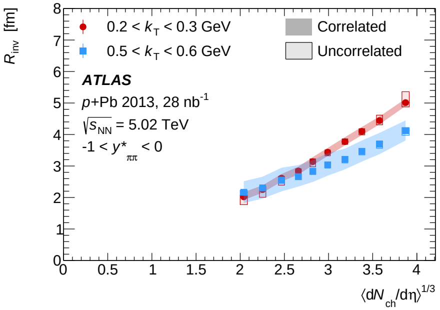

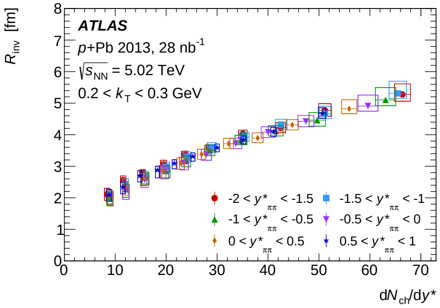

Scaling of R_{inv} with the cube root of average multiplicity curves slightly upward.

Across centrality and rapidity intervals, the source size is tightly correlated with the local multiplicity.
- First such observation

PRC **96** (2017) 064908

Pion identification

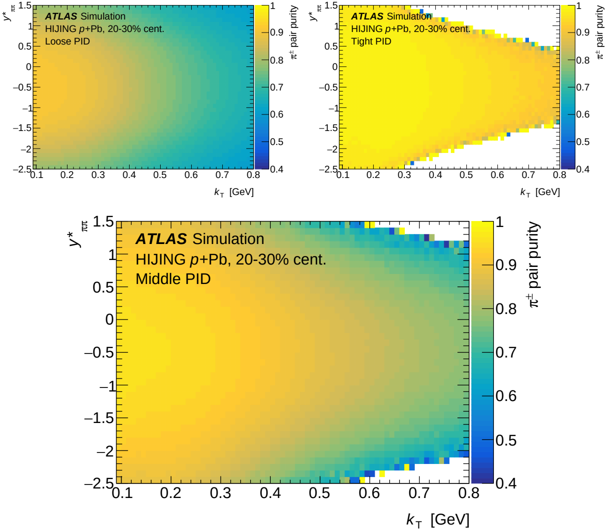

PRC **96** (2017) 064908

Three PID selection criteria are defined, and a variation from the nominal selection to a looser and tigher definition is used as a systematic variation.

Jet fragmentation in opposite-charge HIJING

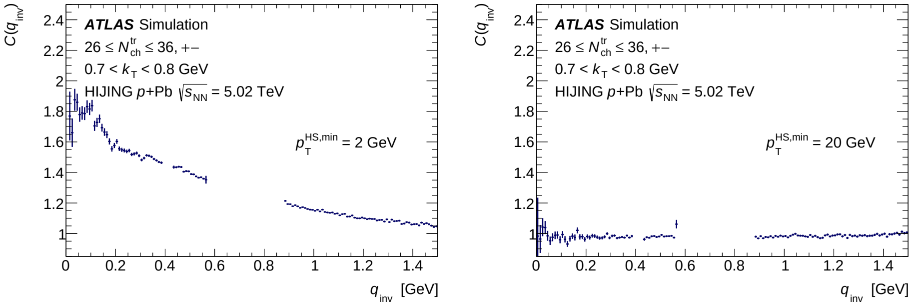

Wide correlation disappears in opposite-charge too when turning off hard processes

Jet fragmentation correlation

A data-driven method is developed to constrain the effect of hard processes. Fits to the opposite-charge correlation function are used to constrain the fragmentation correlation in same-charge. This has its own challenges.

1. Resonances appear in the opposite-charge correlation functions
    - mass cuts around ρ, K_S, and ϕ
    - cut off opposite-charge fit below 0.2 GeV
2. Fragmentation has different effect on the opposite-charge correlation function than on the same-charge
    - a mapping is derived from opposite- to same-charge using simulation
    - opposite-charge fit results in the data are used to fix the background description in the same-charge

Jet fragmentation correlation

The jet fragmentation is modeled as a stretched exponential in q_{inv}:

$$\Omega(q_{\text{inv}}) = 1 + \lambda_{\text{bkgd}}^{\text{inv}} e^{-|R_{\text{bkgd}}^{\text{inv}} q_{\text{inv}}|^{\alpha_{\text{bkgd}}^{\text{inv}}}}$$

In 3D it is factorized into components parallel and perpendicular to jet axis

$$\Omega(\mathbf{q}) = 1 + \lambda_{\text{bkgd}}^{\text{osl}} e^{-|R_{\text{bkgd}}^{\text{out}} q_{\text{out}}|^{\alpha_{\text{bkgd}}^{\text{out}}} - |R_{\text{bkgd}}^{\text{sl}} q_{\text{sl}}|^{\alpha_{\text{bkgd}}^{\text{sl}}}}$$

with $q_{\text{sl}} = \sqrt{q_{\text{side}}^2 + q_{\text{long}}^2}$.
These parameters are studied in Pythia, and a mapping from opposite-charge to same-charge values is derived.

Jet fragmentation mapping (invariant)

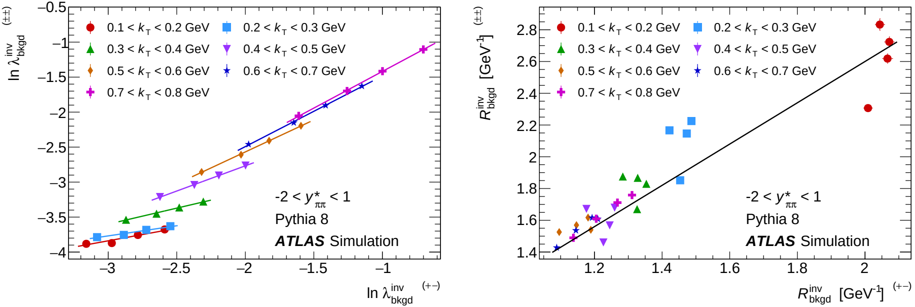

model $R_{\rm inv}^{\pm\pm}$ as proportional to $R_{\rm inv}^{+-}$ (right). Then with constant fixed, do $k_{\rm T}$-dependent comparison of background amplitude in $\pm\pm$ and $+-$ (left). Does not work perfectly but does increasingly well at high $k_{\rm T}$, where the effect is relevant.

Jet fragmentation mapping (3D)

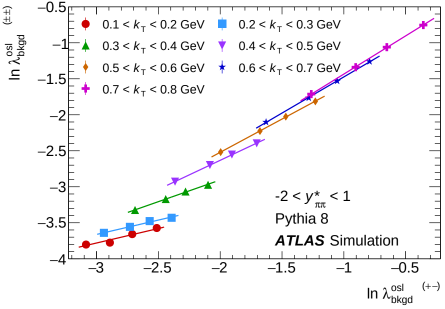

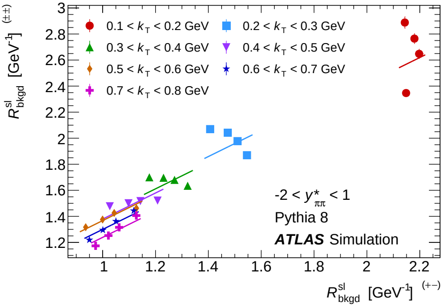

Systematics example (R_{inv})

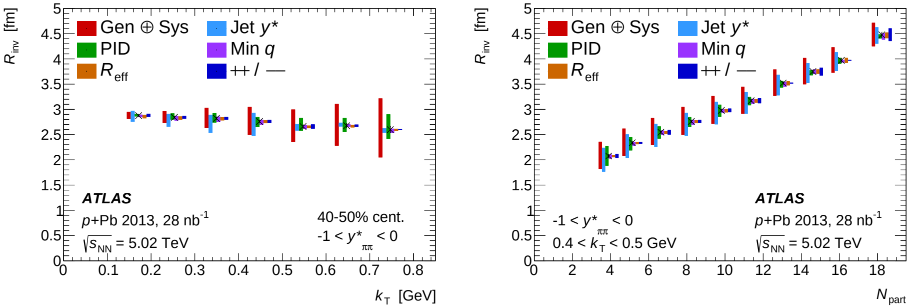

The above plots show the contributions of each systematic uncertainty on R_{inv} as a function of k_{T} and N_{part}.

Systematics example (λ_{inv})

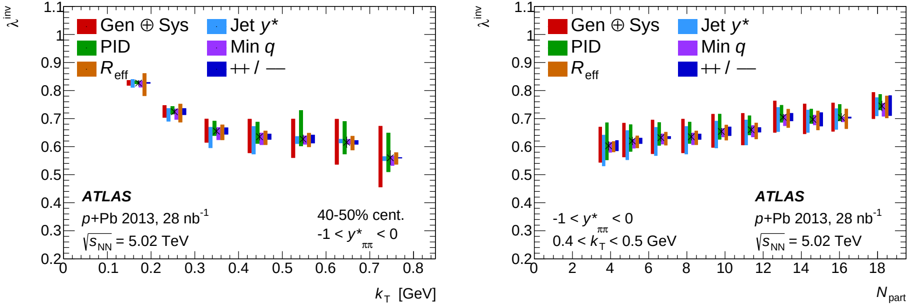

The above plots show the contributions of each systematic uncertainty on λ_{inv} as a function of k_{T} and N_{part}.

Invariant λ

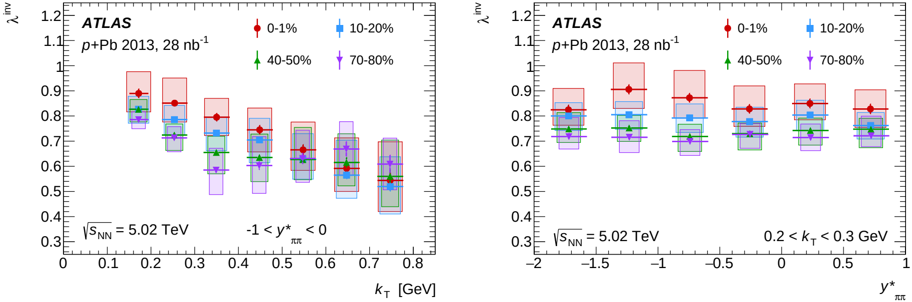

3D λ

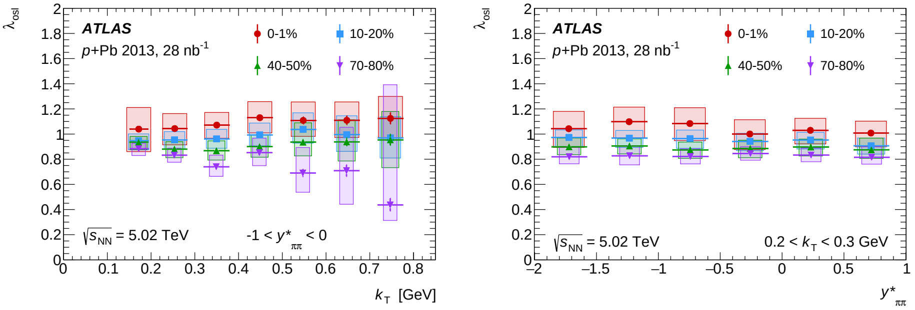

λ_{osl}
ATLAS
p+Pb 2013, 28 nb^{-1}
0-1%
10-20%
40-50%
70-80%
$\sqrt{s_{NN}}$ = 5.02 TeV
$-1 < y^*_{\pi\pi} < 0$
k_T [GeV]
λ_{osl}
ATLAS
p+Pb 2013, 28 nb^{-1}
0-1%
10-20%
40-50%
70-80%
$\sqrt{s_{NN}}$ = 5.02 TeV
$0.2 < k_T < 0.3$ GeV
$y^*_{\pi\pi}$

Azimuthal HBT at RHIC

STAR results as function of centrality (left) and k_{T} (right):

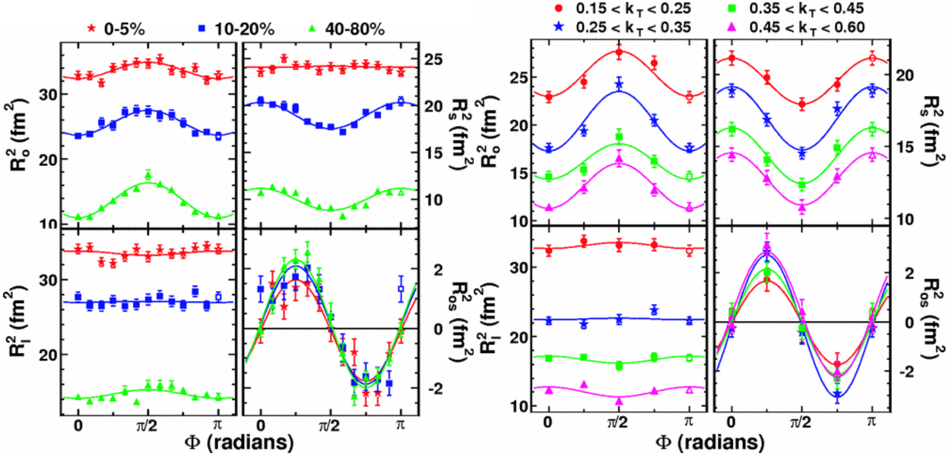

R_{out}/R_{side}: azimuthal dependence

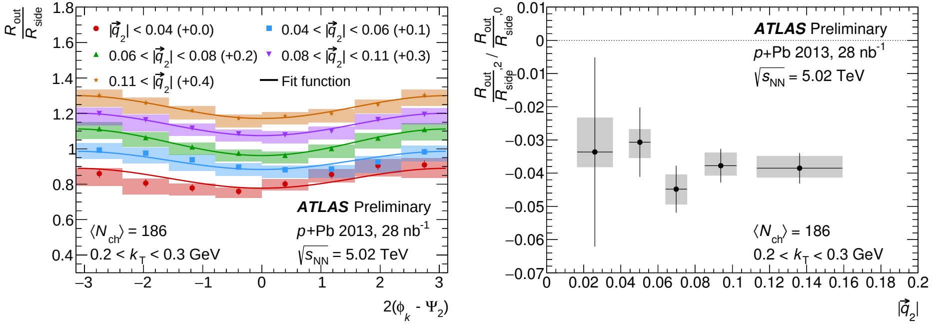

- $$\frac{(R_{out}/R_{side})_{,2}}{(R_{out}/R_{side})_{,0}} \approx \frac{R_{out,2}}{R_{out,0}} - \frac{R_{side,2}}{R_{side,0}}$$

ATLAS-CONF-2017-008